Hot-Pressed Dowels in Bonded-in Rod Timber Connections

Abstract

Bonded-in rod connections are becoming a more and more popular method in the construction industry for connecting timber, favoured for their versatility. The most commonly used system is bonded-in steel rods which are typically prone to have brittle failures. The aim of this study is to investigate the potential of hot-pressed wooden rods as an alternative to conventional steel bonded-in rod systems which have better material harmonisation and excludes the use of adhesives. The proposed connection was applied to practical situation of a beam splice in flexure to determine its potential. The results showed that ductile failure mode was observed at high rotations where peak loads were displayed. A theoretical model was developed and was found to be accurate in comparison to the experimental results. This type of connection has good ductility which suggests its application in domestic timber framing in regions of high seismicity would be practical.

Keywords:

Bonded-in rod, Timber connection, Compressed wood

Introduction

Connections within the framing are usually the critical points of the structure. The choice of connection type and layout is crucial since it will directly affect the global performance of the structure. The construction industry currently uses conventional bonded-in rods which often are responsible for unfavourable brittle failures and have poor environmental credentials. Bonded-in rod connections are becoming a popular connecting method due to their versatility, aesthetic qualities, performance, and economic value (Bainbridge and Mettem 1999). In some areas, such as in Japan, bonded-in rods are very commonly used in housing and residential construction due to the ease of fabrication and excellent performance (Jung et al 2010). They are also becoming more popular in modern European domestic framing, for example, this system has been manufactured in France and used widely in timber framed houses (Ansell and Smedley 2007). A wide range of parameters of steel bonded-in rods connections used in timber members under axial loading have been investigated. Tests have been carried out on spacing and edge distance of steel glue-in rod connections in timber members under axial load to quantify the load carrying capacity (Blass and Laskewitz 1999), the influence of timber density, geometric parameters such as members and rods dimensions have also been studied to prevent premature splitting of the timber members (Gustafsson et al 2001, Feligioni et al 2003, Steiger et al 2007). The conventional steel bonded-in rod connections are prone to exhibit brittle failure in tension or premature splitting due to the disharmonisation between the rod and timber in bending (Yeboah et al 2009). Some systems have tried to address this issue including, for example glass fibre reinforced polymer (GFRP) bonded-in rods was recommended as an alternation of steel GIR connection as they have better compatibility with parent material and adhesive (Harvey 2003). However, GFRP rods are not easy to cut or machine onsite which makes them extremely awkward to recycle when the structures come to the end of their life. Hardwood (Jensen et al 2001) and hot-pressed wooden dowels (Jung et al 2010) are also recommended as alternative solutions to tackle the problems of steel GIR connections. Another problem with all existing GIR systems is the use of adhesives or glues; usually a two part epoxy resin is used. Structural adhesives including

epoxy resin have been associated with causing skin irritation and triggering asthma, which raises health and safety concerns. The use of adhesives requires very good quality control systems so connections are very often manufactured off-site. Some adhesives used in an external environment have also been known to leach into the surrounding eco-system causing deterioration. There is a gap in the industry for an eco-friendly, recyclable and non-brittle alternative to existing GIR systems leading to the development of an all-timber binder-less connection. This study proposes a new system, binderless hot-pressed dowel, to tackle the issues aforementioned and explore the potential of this new system used in a timber framed structure.

Proposed connection

The hot-pressed timber undergoes a thermal-mechano-hydro process; the timber is densified with high temperature. A number of studies have reported stability the hot-pressed timber and how to stabilise them (Welzbacher et al 2008, Rautkari et al 2010, Fang et al 2012). Very limited researches take different approach by exploiting the swelling properties of hot-pressed wood (Anshari et al 2011, Anshari et al 2012). This study relies on friction along the dowel – hole interface caused by the expansion of the soaked dowel within the clearance hole. As the dowel expands it will exert a confining force onto the parent timber hole wall (N_{swell}), which will then mobilises a frictional resistance force (F_{mob}) when the dowel is subject to pull-out (P), shown in Figure 1. Overtime the regular timber dowels will eventually dry-out and shrink alleviating the confining pressure; however, hot-pressed timber dowels retain a portion of expansion caused by swelling which addresses this issue. This connection enables harmony between the two materials which should improve ductile behaviour whilst increasing the recyclability due to the absence of glue and metal. A distinct application could be timber framing in domestic housing, where the connection can be used for header - stud connections and column splicing.

Analytical approach

Figure 2 shows the connections proposed being used as a beam-beam connection under bending. The dowel exhibit flexure (M_d) deformation due to the beam moment (M_{beam}). Where D is the lever arm depth of the dowel from the beam top and the angle of opening is θ_1. The angle of curvature (θ_2) in the dowel may be different to the opening angle of the beam (θ_1) but can be determined using similar triangles and the radius curvature (R_d) as shown in Figure 3:

$$\theta_2 \times R_d = \theta_1 \times D \quad (1)$$

The energy dissipated by the dowel in bending ($U_{d,bend}$) is equal to the moment in the dowel (M_d) multiplied by the rotation of the dowel (θ_2). The energy dissipated by flexure can be written as:

$$U_{d,bend} = M_d \times \theta_2 \quad (2)$$

Combining eqns (1) and (2) gives:

$$U_{d,bend} = \frac{M_d \theta_1 D}{R_d} \quad (3)$$

When consider dowel slipping, the dowel will mobilise frictional slip resistance (F_{mob}) which will increase the joint moment capacity shown in Figure 4.
The frictional force that can be mobilised is related to the normal force on the side of the parent timber hole wall (N_{tot}) and the coefficient of friction between the dowel and wall (μ):

$$F_{mob} = N_{tot} \times \mu$$

(4)

The normal force is made up of two components: the force due to the dowel swelling (N_{swell}) and the forces due to the moment in the dowel (N_{bend}). Figure 5 shows the stress distribution on the parent timber hole wall due to the dowel.
The normal force due to the reaction to the dowel in flexure (N_{bend}) is related to the dowel moment (M_d). The couple caused by N_{bend} is a rection to the moment in the dowel (M_d) and both are equal as given:

$$N_{bend} \times \tfrac{2}{3} l_{eff} = M_d$$

(5)

$$l_{eff} = l - \frac{1}{2} D\theta_1$$

(6)

Combining Eqns (5) and (6) gives:

$$N_{bend} = \frac{3M_d}{2(l - \tfrac{1}{2} D\theta_1)}$$

(7)

The normal force due to swelling is equal to the swelling pressure (f_{swell}) multiplied by the effective length of the dowel (l_{eff}) multiplied by the effective swelling circumference. The effective swelling circumference is equal to half the normal circumference since the dowel only expands in the radial direction not tangentially. The normal force due to swelling can be expressed as:

$$\begin{aligned} N_{swell} &= f_{swell} l_{eff} \tfrac{1}{2} \pi d \\ &= \tfrac{1}{2} f_{swell} (l - \tfrac{1}{2} D\theta_1) \pi d \end{aligned}$$

(8)

The total normal force then becomes the bending and swelling components combined, and can be written as:

$$N_{tot} = \frac{3M_d}{2(l - \tfrac{1}{2} D\theta_1)} + \tfrac{1}{2} f_{swell} (l - \tfrac{1}{2} D\theta_1) \pi d$$

(9)

The total frictional resistance force mobilised (F_{mob}) is then equal to the kinetic coefficient of friction (μ) (since dowel has already started slipping) multiplied by this normal force (N_{tot}):

$$F_{mob} = \mu \frac{3M_d}{2(l - \tfrac{1}{2} D\theta_1)} + \tfrac{1}{2} \mu f_{swell} (l - \tfrac{1}{2} D\theta_1) \pi d$$

(10)

The energy dissipated by the dowel slipping ($U_{d,slip}$) is equal to the frictional force (F_{mob}) multiplied by the slip displacement of the dowels. Assuming the angles are small, the energy Dissipated from slipping can be written as:

$$U_{d,slip} = F_{mob} \times D\theta_1 \quad (11)$$

Combining Eqns (10) and (11) gives:

$$U_{d,slip} = \mu \frac{3M_d D\theta_1}{2(l - \frac{1}{2} D\theta_1)} + \frac{1}{2} \mu f_{swell} l D \theta_1 \pi d \quad (12)$$

The overall energy dissipated by the connection during bending (U_{tot}) is the two components combined, and can be written as:

$$U_{tot} = \frac{M_d \theta_1 D}{R_d} + \mu \frac{3M_d D\theta_1}{2(l - \frac{1}{2} D\theta_1)} + \frac{1}{2} \mu f_{swell} l D \theta_1 \pi d \quad (13)$$

If we consider conservation of energy then work done equals the total energy dissipated during failure:

$$M_{Rd}\theta_1 = \frac{M_d \theta_1 D}{R_d} + \mu \frac{3M_d D\theta_1}{2(l - \frac{1}{2} D\theta_1)} + \frac{1}{2} \mu f_{swell} l D \theta_1 \pi d \quad (14)$$

Assuming the angle is small, the moment capacity of beam can be expressed in the form of:

$$M_{Rd} = M_d D \left(\frac{1}{E_d I_d} + \mu \frac{3}{2l} \right) + \frac{1}{2} \mu f_{swell} l D \pi d \quad (15)$$

Experiments

Dowel bending tests

Red Western cedar (*Thuja plicata*) with average density of 390kg/m^3 was used to fabricate hot-pressed dowels and as specimens in bending, punching shear and beam bending tests. To hot-press timber, the wood specimens were then placed between platens which were pre-heated to 130^{o}C and pressed for 5 minutes with compression ratio of 40%. The compression ratio can be defined as:

$$C = \frac{R_0 - R_C}{R_0} \times 100[\%] \quad (16)$$

Where R_0 and R_c, respectively represents dimension in compression direction before and after compressed, respectively.

Four point bending tests were conducted to establish the mechanical properties of the hot-pressed dowels. To have a more reliable results and less variation, a total of 30 hot-pressed specimens were then cut into dimensions of 12x12x240mm for bending tests. The specimens prepared for the bending test have the averaged density of 553.2 kg/m^3 with a standard

deviation of 62.0 kg/m^3. The effective span between supports was set to be 200mm. All testing procedures and determination of mechanical properties were conducted in compliance with BS EN 408:2010 (BSI 2011).

Punching Shear Tests

Punching shear tests were conducted in order to determine the performance of the bond between parent timber and expanded dowel. Clear and small Red Western cedar samples with dimensions of 23 x 15 x 260mm were prepared and hot-pressed from 23mm to 14mm thick. Two series of specimens were prepared for punching tests, series A and B. The specimens of the series A were left for 4 days to allow for spring back then shaved into 12mm diameter circular dowels using a lathe. The specimens in the series B were shaved into 12mm diameter round dowels right after the completion of hot-press process. Parent specimens of spruce 75 x 75mm were then prepared with 12mm diameter centre holes longitudinal to the grain; water was injected into the hole before the dowels were inserted. This will result in two different level of swelling of hot-pressed dowels.
The completed samples were then sliced into punching shear specimens as shown in Figure 6. Thicknesses tested include 10, 20, 30, 50, 80, 100 and 150mm. A total of 5 tests were conducted for each group with different thickness which makes up 70 specimens for punching tests. The specimens were left 4 days before testing to allow the dowels to dry. The punching shear tests were conducted using a customised rig and a DARTEC 100 kN test machine with a rate of 0.5mm/min. Tests were conducted up to the point where the dowel was completely punched out or up to a 10mm slip displacement. The overall test set-up is illustrated in Figure 7.

Time-dependent shear tests

To investigate the relationship between shear strength versus time, a series of punching shear tests were carried out on Type B specimens 2, 48, 168, 720, and 2160 hours after the specimens were prepared. The thickness of the specimens is 10mm, and five specimens were tested for each time span. This series of specimens were tested with the same condition with punching shear tests.

Beam tests

A hot pressed dowel was used to connect two pieces of timber with dimensions of 75x150x600mm to build a beam with length of 1.2m. A total of 24 specimens were fabricated for bending tests. Grade C16 European whitewood (*Picea abies*) was used as the parent beam material. The embedment length was kept constant at 100mm each end (200mm total dowel length). The averaged moisture content of the beam specimens was 12% measured by moisture metre before the tests.
The factors investigated in this study include edge distance and types of dowels. The edge distance is defined as the distance between the beam soffit and the placement of the dowel centre within the section. The edge distances tested include: 2d (24mm), 3d (36mm), 4d (48mm) and 5d (60mm); where d is the dowel diameter. Two types of dowels, as explained in punching shear tests were used to connect beam specimens. Three repetitions were tested with each factor combination. Table 1 gives the name and details of each specimen. The specimens and the test setup are explained in Figure 8.

Results and Discussions

Bending tests

The results of bending tests have shown an average Modulus of Elasticity (MOE) of 13.86kN/mm^2 with a standard deviation of 0.41kN/mm^2, which is comparable to timber with strength class of C35 ($E_{0,mean}$=13 kN/mm^2). Based on BS EN 14358:2006 (BSI 2007), the 5% MOE ($E_{0.05}$) is 12.81 kN/mm, which is comparable to timber with strength class of C50 (11 kN/mm^2), this shows the MOE has increased by two times compared with strength class C16 after the hot-pressed process and also demonstrates that hot-pressed process can be a useful method to enhance the mechanical properties of low grade timber.
The results have also shown that the hot-press process significantly increase the bending strength of the low grade timber. The characteristic bending strength of the hot-pressed timber was 66.5 kN/mm^2, which is higher than the characteristic bending strength of C50 timber and comparable to D60 hardwood.

Punching shear tests

The results of punching shear tests are summarised in Table 2, and Figure 9 plots the maximum shear stress against specimen thickness. The maximum averaged shear stress was calculated by:

$$\tau_{av,peak} = \frac{P_{max}}{\pi \cdot d \cdot l} \tag{17}$$

where $P_{max}, d, and\ l$ are peak force when dowels are mobilised, the diameter of dowel, the length of dowel, respectively. It can be found that the specimens in series B show much higher peak values, and in consequence lead to higher averaged maximum shear stresses. It is because the series B hot-pressed dowels did not spring back before they were inserted into the holes in beam members. The swellings started due to the water in the holes after dowels were inserted into but confined by the holes. In comparison, the dowels in series A have sprung back before they were shaved into dowels, therefore exhibit limited swelling even being soaked in water in the holes of beam members.
It was observed that Initially the maximum averaged shear stress was found to decrease rapidly as specimen thickness increases but this relationship starts levelling off near 100mm for series A dowels and 50mm for series B dowels. After these thickness levels there are no significant decrease in maximum averaged shear stress; this is compliant with existing bonded-in rod theory (Volkersen 1953).

Time-dependent shear strength

The friction between dowels and parent timber relies on the swelling of compressed wood, therefore drying of dowel and parent timber influence the punching shear over time. Figure 10 depicts the relationship between shear strength and time after the specimens were fabricated. It shows that the averaged punching shear strength of the specimens decreases over time, however, 2 days after the specimens were prepared, the shear strength did not show significant change. The shear strength of the specimens is 0.42 and 0.39 N/mm^2 for 2 and 90 days after fabrication, respectively. These represent 22 and 27% of reduction when compared with 2 hours after the specimens were made.

Beam bending tests

Two different failure modes were observed in the beam tests, being brittle and ductile failures. Observations from experimental results have shown that 9 out of 12 beam specimens

connected with series A dowels and 10 out of 12 specimens connected with series B dowels have exhibited ductile failure. This implies that beam connected with hot-pressed dowels normally fail in ductile mode, which is normally preferred for a structural application to avoid catastrophic collapse of structures.

Specimens that failed in a ductile manner seemed to partially snap forming an intact hinge at peak moment. Post peak the connection showed around half the moment capacity when the dowel seemed to provide purely frictional resistance by sliding out of the clearance holes. The ductility appears to be provided by this frictional resistance; a large portion due to the swelling of the dowel and this is particularly obvious when the beam specimens are connected by series B dowels. This also indicates that more swelling provides higher post peak residual strength.

The brittle specimens typically had higher moment capacities than that of a ductile counterpart. In this case the dowel does not form a hinge and suddenly snaps at the maximum moment capacity showing no post peak ductility.

The density of the dowels was measured before the tests and it was found that the denser dowels were responsible for the brittle specimen failures. This means that using denser dowels will lead to more brittle failures due to the inability to form early hinges and access the residual frictional resistance. All the dowels were taken from the same piece of timber so these differences in density maybe due to the presence of juvenile wood along the timber length. Figure 11 plots the ultimate strength of beams connected by the two series of dowels against the density of the dowels. It was found that those specimens connected by dowels with density higher than 700kg/m^3 exhibit failure in brittle manner. For structural application lower density dowels (below 700kg/m^3) will help to ensure a ductile failure. A quality control procedure will also be required to monitor dowel density before and after hot-pressing which can fluctuate substantially (Kitamori et al 2010).

Table 3 summarises the beam test results, which shows: maximum moment capacity, initial rotational stiffness, rotation at peak and rotation at failure. The results show that the smaller the edge distances are, the higher the ultimate strength the beam will have. The beams connected by series B dowels have significantly higher ultimate strength compared with those connected by series A dowels. This also reflects the fact that the punching shear strengths of series B dowels are higher than those of series A dowels. The above two phenomenon will be explained in the analytical model later in this article.

Comparison with analytical model

The analytical model has been developed earlier in this paper using energy method; the moment capacity of beams can be calculated by Eqn (15). The comparisons between estimated strength with those obtained from experiments are given in Figure 12. Satisfactory agreement was found between analytical and experimental results, with those beams connected with type A dowels have more errors compared with those with type B dowels.

Conclusions

The proposed connection system was used in a beam splice connection; bending tests were carried out to assess its performance in a practical application. Modest moment capacities in the region of 0.055 – 0.085 kNm was observed for specimens with type A dowel and 0.16-0.24 kMm was observed in the specimens with type B dowel. All the specimens showed very high rotations at failure around 0.30 – 0.35 radians (17 – 20^{o}) which is favourable for structural applications to provide early pre-collapse warning.

References

Bainbridge R, Mettem C (1999) Bonded-in rods for timber structures: a versatile method for achieving structural connections. Structural Engineer **77**(15): 24-27
Jung K, Murakami S, Kitamori A, Chang W-S, Komatsu K (2010) Improvement of glued-in-rod joint system using compressed wooden dowel. Holzforschung **64**(6): 799-804
Ansell M, Smedley D (2007) Briefing: Bonded-in technology for structural timber. Proceedings of the ICE-Construction Materials **160**(3): 95-98
Blass H, Laskewitz B (1999) Effect of spacing and edge distance on the axial strength of glued-in rods. CIB-W18 Meeting 32 Graz, Austria, Universität Karlsruhe.
Gustafsson P, Serrano E, Aicher S, Johansson C (2001) A strength design equation for glued-in rods. Proceedings of the international RILEM symposium on joints in timber structures. Aicher S and Reinhardt H. Eds. RILEM, Stuttgart, Germany.
Feligioni L, Lavisci P, Duchanois G, De Ciechi M, Spinelli P (2003) Influence of glue rheology and joint thickness on the strength of bonded-in rods. Holz als Roh-und Werkstoff **61**(4): 281-287
Steiger R, Gehri E, Widmann R (2007) Pull-out strength of axially loaded steel rods bonded in glulam parallel to the grain. Materials and structures **40**(1): 69-78
Yeboah D, Gilbert S, Gilfillan R (2009) The behaviour of moment-resisting timber joints using bonded steel rods. Proceedings of the 11th International Conference on Non-conventional materiails and Technologies (NOCMAT). Walker P, Ghavami K, Paine K, Heath A, Lawrance M and Fodde E. Eds. University of Bath, Bath, UK.
Harvey K (2003) Improved timber connections using bonded-in GFRP rods. PhD Thesis, University of Bath. Bath, UK.
Jensen J, Koizumi A, Sasaki T, Tamura Y, Iijima Y (2001) Axially loaded glued-in hardwood dowels. Wood science and technology **35**(1-2): 73-83
Welzbacher C, Wehsener J, Rapp A, Haller P (2008) Thermo-mechanical densification combined with thermal modification of Norway spruce (Picea abies Karst) in industrial scale–Dimensional stability and durability aspects. Holz als Roh-und Werkstoff **66**(1): 39-49
Rautkari L, Properzi M, Pichelin F, Hughes M (2010) Properties and set-recovery of surface densified Norway spruce and European beech. Wood science and technology **44**(4): 679-691
Fang C-H, Mariotti N, Cloutier A, Koubaa A, Blanchet P (2012) Densification of wood veneers by compression combined with heat and steam. European Journal of Wood and Wood Products **70**(1-3): 155-163
Anshari B, Guan Z, Kitamori A, Jung K, Hassel I, Komatsu K (2011) Mechanical and moisture-dependent swelling properties of compressed Japanese cedar. Construction and Building Materials **25**(4): 1718-1725
Anshari B, Guan Z, Kitamori A, Jung K, Komatsu K (2012) Structural behaviour of glued laminated timber beams pre-stressed by compressed wood. Construction and Building Materials **29**: 24-32
BSI (2011) BS EN 408: 2010 Timber structures–Structural Timber and Glued Laminated Timber–Determination of Some Physical and Mechanical Properties. British Standards Institute. London.
BSI (2007) BS EN 14358:2006 Timber structures. Calculation of characteristic 5-percentile values and acceptance criteria for a sample British Standards Institute. London.
Volkersen O (1953) Die Schubkraftverteilung in Leim-, Niet-und Bolzenverbindungen. Energie und Technik **5**(68): 103
Kitamori A, Jung K, Mori T, Komatsu K (2010) Mechanical properties of compressed wood in accordance with the compression ratio. Mokuzai Gakkaishi **56**(2): 67-78 (In Japanese).

List of Figures

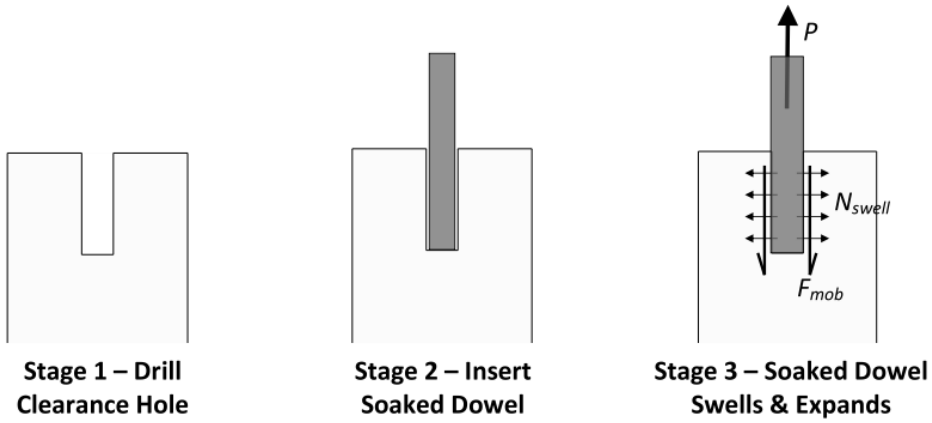

Figure 1. Principle of Proposed Connection

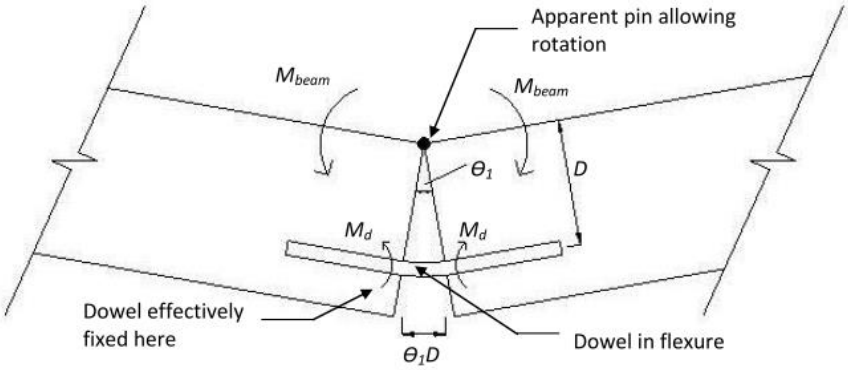

Figure 2. Contribution from Dowel in Bending

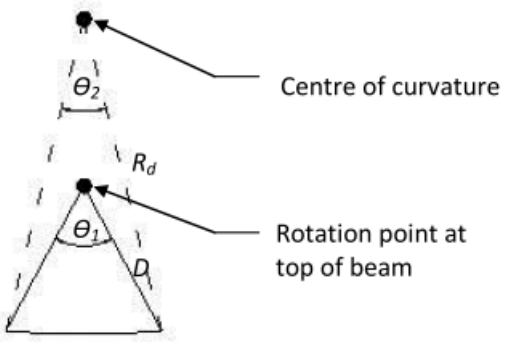

Figure 3. The relationship of curvature and rotation centre of beam

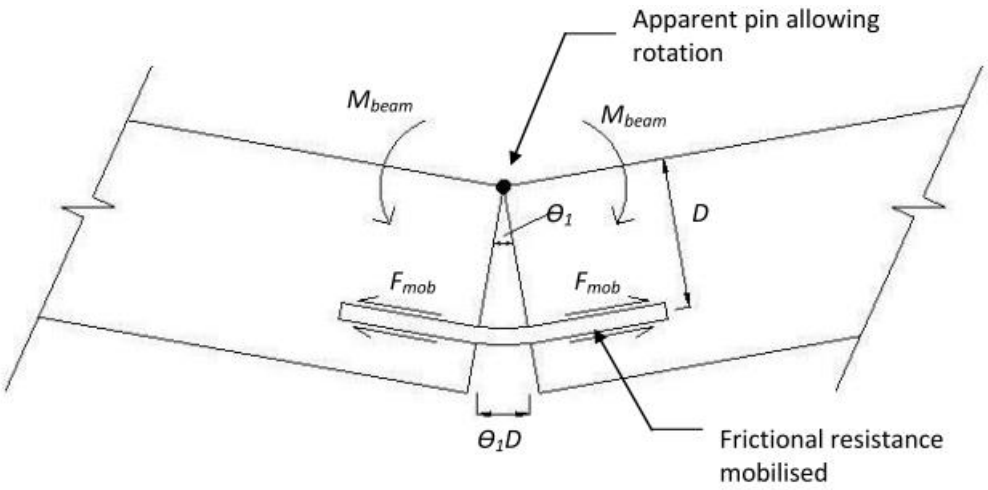

Figure 4. Contribution from Dowel Slipping

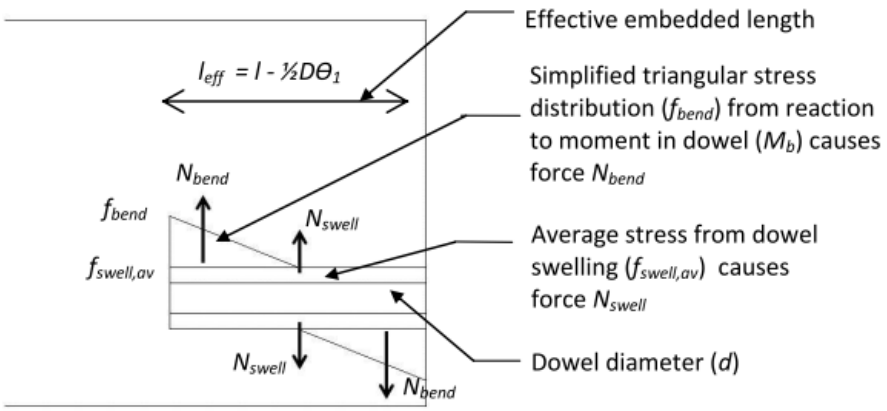

Figure 5. Stress Distribution on Dowel Hole during Slippage

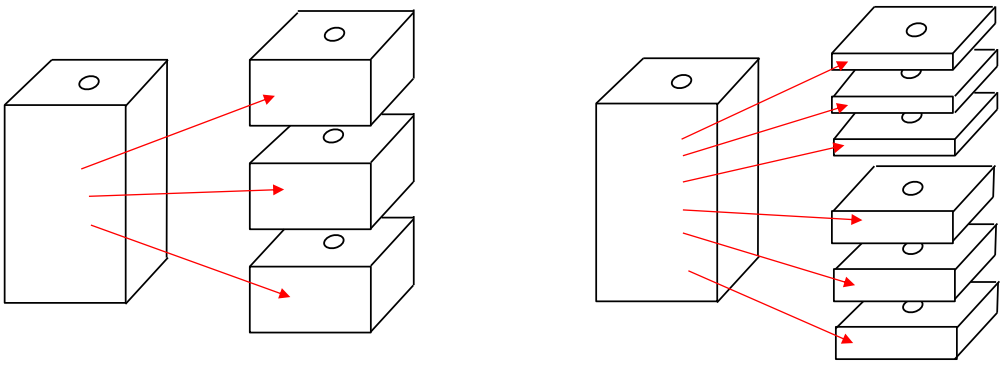

Figure 6. Punching shear specimen slicing preparation for 10, 20 and 30mm thickness specimens

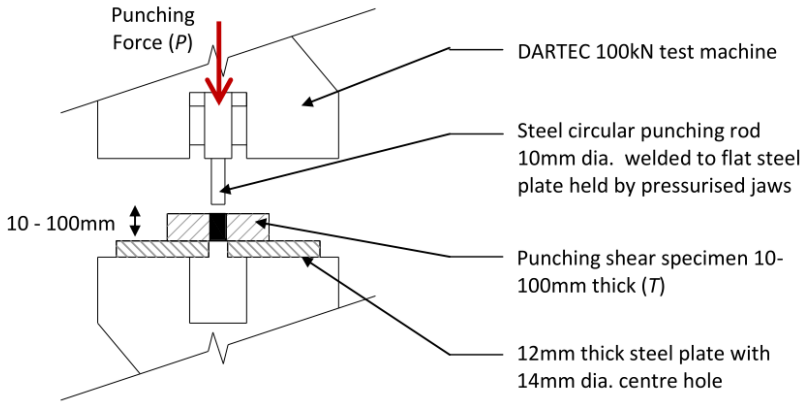

Figure 7. Punching shear test setup

Figure 8. Beam bending test setup

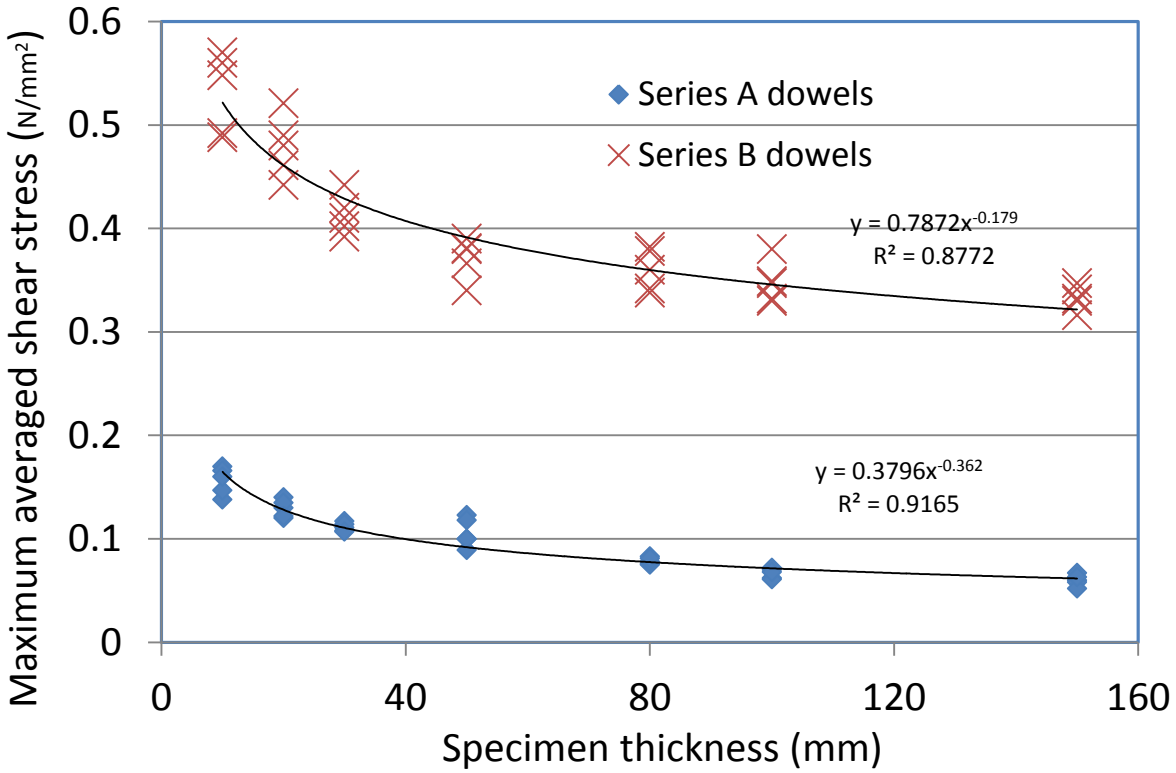

Figure 9. Average Shear Stress at Peak Load vs. Specimen Thickness

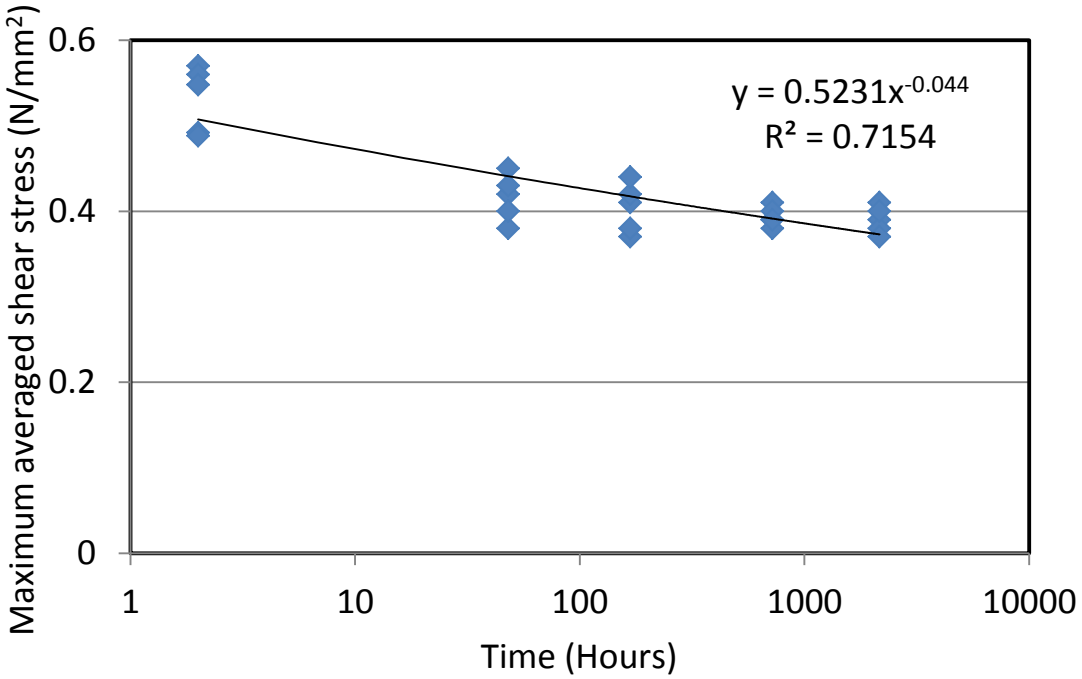

Figure 10 Average Shear Stress at Peak Load of 10mm thickness specimen versus time after fabrication

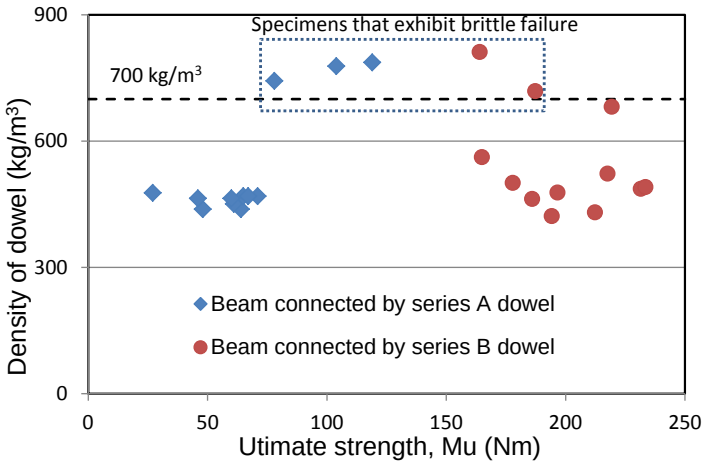

Figure 11. Density of hot-pressed dowel versus ultimate bending capacity of beam

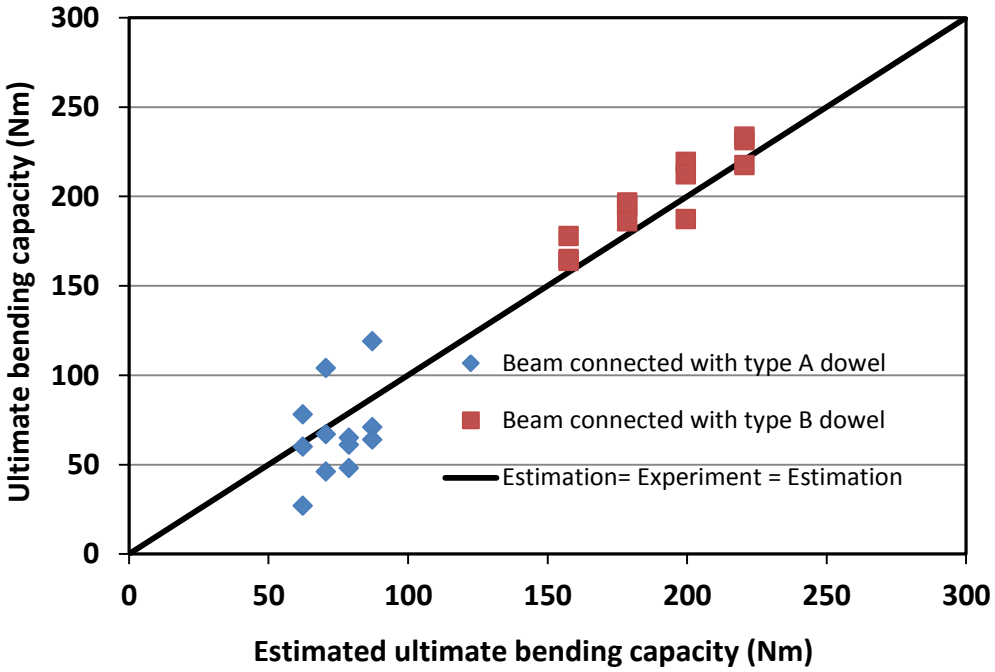

Figure 12. Comparison of results from estimation and experiments

Table 1. Parameters for beam bending tests

Specimens	type of dowel[1]	edge distance	No. of specimens
A-2d	A	2d	3
A-3d	A	3d	3
A-4d	A	4d	3
A-5d	A	5d	3
B-2d	B	2d	3
B-3d	B	3d	3
B-4d	B	4d	3
B-5d	B	5d	3

[1] "A" represents the same process of dowels in group A in punching shear tests; whereas "B" means the B group.

Table 2. Results for punching shear tests

Specimens series	Averaged P_{max} (N)	Maximum averaged Shear stress, $\tau_{av,\,peak}$ (N/mm^2)	Specimens series	Averaged P_{max} (N)	Averaged maximum Shear stress, $\tau_{av,\,peak}$ (N/mm^2)
A-10	58.89 (5.05)[1]	0.156 (0.013)	B-10	200.41 (14.62)	0.532 (0.039)
A-20	97.57 (6.39)	0.129 (0.008)	B-20	361.01 (22.55)	0.479 (0.030)
A-30	125.99 (4.70)	0.111 (0.004)	B-30	467.32 (21.61)	0.413 (0.019)
A-50	199.81 (26.56)	0.106 (0.014)	B-50	700.07 (36.83)	0.371 (0.020)
A-80	237.05 (10.14)	0.079 (0.003)	B-80	1085.73 (60.62)	0.360 (0.020)
A-100	251.08 (18.39)	0.067 (0.005)	B-100	1310.42 (75.52)	0.348 (0.020)
A-150	339.29 (31.74)	0.060 (0.006)	B-150	1884.20 (66.84)	0.333 (0.012)

[1] *standard deviations shown in brackets*

Table 3. Results for beam tests

Specimens	Ultimate strength M_{ult} (Nm)	Initial Rotational Stiffness k_i (kNm/rad)	Rotation at Peak Moment Θ_{peak} (rads)	Rotation at Failure $\Theta_{failure}$ (rads)
A-2d	84.67 (29.94)[1]	2.76 (3.08)	0.14 (0.07)	0.27 (0.05)
A-3d	58.00 (8.89)	2.78 (1.46)	0.11 (0.04)	0.34 (0.04)
A-4d	72.33 (29.37)	1.01 (0.34)	0.16 (0.12)	0.34 (0.04)
A-5d	55.00 (25.87)	0.75 (0.33)	0.25 (0.13)	0.37 (0.02)
B-2d	227.48 (8.68)	6.32 (1.03)	0.18 (0.06)	0.33 (0.04)
B-3d	206.26 (16.85)	5.87 (1.52)	0.16 (0.02)	0.36 (0.01)
B-4d	192.27 (5.57)	3.63 (0.73)	0.20 (0.08)	0.29 (0.06)
B-5d	168.88 (7.73)	2.88 (0.47)	0.14 (0.04)	0.26 (0.03)

[1] *standard deviations shown in brackets*